ELSEVIER

Polymer 43 (2002) 4495–4502

polymer

www.elsevier.com/locate/polymer

The variability and interdependence of spider drag line tensile properties

M.A. Garrido[a], M. Elices[a,*], C. Viney[b], J. Pérez-Rigueiro[a]

[a]*Departamento de Ciencia de Materiales, Universidad Politécnica de Madrid, ETS de Ingenieros de Caminos, Ciudad Universitaria, 28040 Madrid, Spain*
[b]*Department of Chemistry, Heriot-Watt University, Edinburgh, Scotland EH14 4AS, UK*

Received 14 February 2002; accepted 3 April 2002

Abstract

There is considerable interest in producing fibres that mimic the impressive tensile properties of spider drag line silk. It must, however, be recognised that these properties have been assessed largely on the basis of their average values; there can be significant variability about these averages. The natural variability can also serve as a useful indicator of the range of values over which particular properties of biomimetic silk may be tailored. Here we quantify several tensile properties of drag line from *Argiope trifasciata* spiders. We distinguish between two groups of properties on the basis of their statistical coefficient of variation. There is significantly greater scope for tailoring the viscoplastic hardening aspects of drag line, compared to the variability of the initial elastic response or the yield strength. We also consider whether elastic modulus, yield strength and viscoplastic hardening can be controlled independently of one another.

Keywords: Elastic modulus; Spider silk; Strength

1. Introduction

Spiders use their drag line—primarily fibre produced from the contents of the major ampullate glands—to make safe descents and to build the frames of orb webs. In fulfilling these demanding functions, the drag line achieves a combination of optimised strength and elongation unrivalled by artificial fibres [1,2]. Consequently, there is a widespread interest in mimicking natural silks in order to produce new classes of high performance materials [3].

In tensile tests of drag line, the initial elastic response is succeeded by yield, which in turn is followed by a significant regime of (strain) hardening [4]. A full description of the stress–strain behaviour of drag line therefore requires several parameters. However, characterisation of these properties is usually hampered by their marked variability, which is apparent even when fibres are tested under nominally identical conditions [5–8]. Although the *mean* values of initial stiffness, tensile strength, and elongation to failure are impressively high, individual results can deviate significantly from these means. The magnitude of the variability is a complicating factor in attempts to control selected mechanical properties artificially. For example, infiltration with a cross-linking agent can appear to affect the stress–strain response of drag line, but the changes are statistically insignificant in relation to the intrinsic variability of the response [6]. The variability also masks any structure–property dependence that might be learned by studying the drag line produced by distinct species from unique habitats.

The variability of a given type of silk arises at several levels. First, there is the *interspecific* level, where differences in composition and therefore properties are observed in a given type of silk (e.g. drag line) as produced by distinct spider species [8–11]. Next, there is *intraspecific* variability [8], referring to variations in the mechanical properties of silk obtained from different individuals that belong to the same species. Finally, one must recognise variability at the *intraindividual* level [8,12], i.e. variations between samples obtained from a single individual. The intraspecific and intraindividual scatter can exceed a factor of 2, which is comparable in magnitude to the interspecific variability [8]. It is likely that both the intraspecific and intraindividual variabilities are strongly influenced by the processing of silk, since (i) the properties depend on the rate at which the fibre is spun [13,14], (ii) the flow of silk through the spinneret can be controlled by the spider [8], and (iii) the properties of drag line collected from vertically climbing spiders differ markedly from the properties of drag line spun when the same spiders crawl on a horizontal surface [15]. In addition, it has been suggested recently that these variabilities may in part be related to compositional changes of the protein as secreted in the gland [12].

In terms of spider survival ability, the variability of silk

* Corresponding author. Tel.: +39-91-5433974; fax: +34-91-5437845.
E-mail address: melices@mater.upm.es (M. Elices).

0032-3861/02/$ - see front matter
PII: S0032-3861(02)00254-9

can be regarded as a desirable attribute. It allows production of a material that meets the general requirements imposed by the distinctive environment inhabited by each spider species (interspecific level), and it allows production of silk fitted to the immediately particular requirements of the individual (intraspecific and intraindividual levels). The scope for variability might offer analogous advantages when silk-like artificial fibres are processed, allowing fibre properties to be tailored minutely for the intended use. In other words, the variability, if properly characterised and exploited, can become a user-controlled aspect of artificial fibre spinning. We have therefore addressed the objective of quantifying, and establishing constraints on, the intraspecific/intraindividual variability of spider drag line, i.e. those levels of variability that are most attributable to processing.

Our approach consists of four steps:

1. Selection of a trial set of parameters to describe the stress–strain curves obtained from each of several silk samples.
2. Use of statistical tools on the results from a representative number of tensile tests to determine the variability of these parameters.
3. Determination of which of the parameters are statistically correlated (dependent), and which are statistically independent. This issue is especially relevant to the quest for producing fibres of silk from transgenic sources [3,16,17], since it identifies which properties may be controlled independently in a biomimetic spinning process.
4. Refinement of the trial set, retaining the minimum number of independent parameters that will allow the stress–strain curves to be described (reconstructed) to an acceptable level of accuracy.

2. Experimental

We are concerned here with the tensile properties of naturally spun material, i.e. collected from the web or from the drag line laid down by a crawling spider; we do not use silk obtained by forced reeling. Although drag line spun by spiders crawling horizontally is less reproducible than the silk produced during a vertical climb [15], we use the former material here because we are interested in the degree to which tensile properties *can* be varied in the naturally spun material.

Two *Argiope trifasciata* spiders were kept in boxes 70 cm × 70 cm × 20 cm and fed on a diet of crickets. Silk from one spider (At1) was harvested directly from the web as explained elsewhere [7]. The other spider (At2) was allowed to crawl on a horizontal wooden surface, from where the drag line could be collected carefully with tweezers [15].

Samples of silk were cut and mounted on cardboard frames for tensile testing as described previously [7,15,18,19]. The gauge length for the tests was 20 mm. Tensile property characterisation was performed with an Instron 4411 operating at constant cross-head speed to achieve a nominal strain rate of 0.0002 s^{-1}. Applied load was measured with an electronic balance (AND HF-1200 G, resolution ±10 mg) attached to the lower end of the sample. The cross-head displacement was taken as a direct measurement of the sample deformation, since the compliance of the silk is approximately 1000 times larger than that of the equipment [18]. The tests were performed in air, nominally at 20 °C and 60% relative humidity.

After tensile testing, some samples were retrieved and sputtered with gold. A JEOL 6300 scanning electron microscope was used to measure sample diameters; four measurements were performed in each case [7,18]. The beam voltage and current were 10 kV and 0.06 nA, respectively. Initial sample cross-sectional areas were calculated from these measurements, assuming that sample volume is conserved during the tensile tests [7,18]. The cross-sectional areas were needed to re-scale force–displacement plots as engineering stress–strain curves. It has been demonstrated previously [7,20], and was confirmed in the present study, that adjacent samples cut from the same piece of drag line exhibit closely comparable behaviour in tensile tests. Therefore, we used the cross-sectional areas derived from our SEM measurements to re-scale the force–displacement plots of adjacent samples as well. For this reason, our explicit results for cross-sectional geometry characterisation refer to a smaller number of samples than our results for tensile property characterisation.

3. Results and discussion

3.1. Cross-sectional geometry of silk samples

Results obtained from samples of drag line spun by each spider are summarised in Table 1, where the average monofilament diameter, D_{mean}, maximum diameter, D_{max}, minimum diameter, D_{min}, and average shape anisotropy are presented. The shape anisotropy is an indicator of departure from a circular cross-section [7,19]. Provided that the shape anisotropy is less than 1.2 [19], the sample cross-section is closely approximated by a circle having as its diameter the average of the experimentally measured diameters [21]. Also, for each of the samples that we characterised by SEM, the four measurements of diameter differed by less than 5%. The relative uniformity of cross-sectional geometry exhibited by these naturally spun samples contrasts with the highly variable cross-section of drag line obtained by forced silking of spiders [5,6].

3.2. Intraspecific versus intraindividual variability

We recognised earlier that the variability of silk produced by specimens of the same species has to be considered at two complementary levels: intraspecific and intraindividual. The intraspecific level assumes that each spider *may*

Table 1
Geometrical properties of naturally spun spider silk

Spider	Number of samples	D_{mean} (μm)	D_{max} (μm)	D_{min} (μm)	Average shape anisotropy
At1[a]	13	6.6 ± 0.2	8.5	5.0	1.05 ± 0.01
At2[b]	9	3.5 ± 0.3	4.3	2.7	1.04 ± 0.03

[a] Silk collected from web.
[b] Silk collected from spider crawling on horizontal surface.

produce a set of silk fibres with fixed mechanical properties, and that this set differs from those produced by other spiders of the same species. The actual variation in properties within the set of silk fibres produced by a single spider corresponds to the intraindividual variability. Therefore, it is appropriate to check whether the drag line produced by different spiders exhibits significantly different behaviour. Fig. 1 shows several representative stress–strain curves for drag line from the two spiders used in our study. No consistent differences are apparent between the two sets, i.e. there is no indication that one spider produces fibres with characteristics that cannot be found in fibres produced by the other spider—despite our use of different collecting techniques in the two cases. Consequently, the observed variability can be assigned to the intraindividual level, and all 31 stress–strain curves for drag line from the two spiders are treated as a single set in the statistical analysis which follows.

3.3. Statistical analysis: parameterisation of stress–strain curves

Our statistical analysis requires a set of parameters that allow a functional description of the stress–strain curves, so that any experimental curve can be reconstructed from just those parameters. The initial set of parameters relies on a somewhat arbitrary choice, based on the qualitative features of the stress–strain curves. This initial set can then be expanded or reduced by an iterative process in which the agreement between experimental and reconstructed curves is assessed.

Three regions can be distinguished in a typical stress–strain curve of drag line, as shown in Fig. 2: an initial linear elastic region (A), a yield region (B), and a hardening region where stress increases non-linearly with strain (C). Based on Fig. 2, a workable initial set of parameters for describing the stress–strain curve is:

1. Elastic modulus, E.
2. Yield stress, σ_y (conventional proof stress or offset stress [22], defined at 0.2% strain).
3. Stress at 5% strain, $\sigma_{5\%}$.
4. Stress at 15% strain, $\sigma_{15\%}$.
5. Stress at 25% strain, $\sigma_{25\%}$.
6. Tensile strength σ_u.

Yield stress is preferred here to the proportional limit (another conventional parameter which can be used to define the extent of the elastic region) [7,19,22], because σ_y sustains a better fit to the local maximum at the end of the elastic region. The parameter $\sigma_{5\%}$ is chosen because it consistently lies within the approximately flat section of the yield region. The hardening region, which is non-linear, cannot be represented by a single parameter; we tentatively

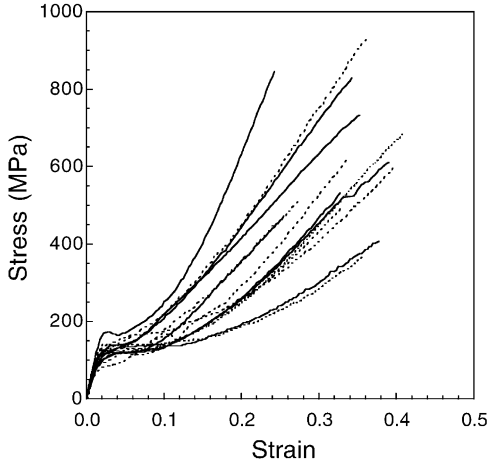

Fig. 1. Stress–strain curves for *A. trifasciata* drag line. Solid lines refer to silk from spider At1 (material was harvested from the web); broken lines refer to silk from spider At2 (material was collected after it was deposited on a horizontal surface by a crawling spider).

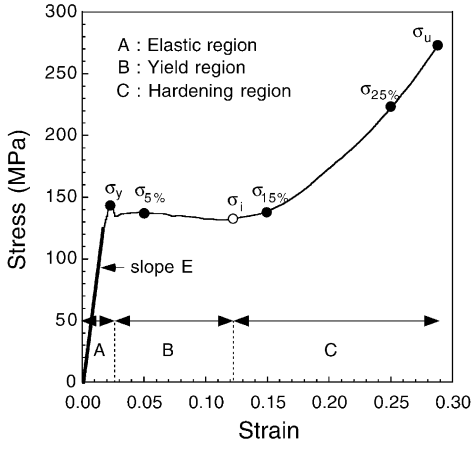

Fig. 2. Regions (A–C) and parameters (E, σ_y, $\sigma_{5\%}$, $\sigma_{15\%}$, $\sigma_{25\%}$, σ_u) used to describe the stress–strain curves of *A. trifasciata* drag line, as defined in the text. The stress σ_i is defined as the point where the yield region ends and the hardening region begins; the method for determining its location is described in Appendix A.

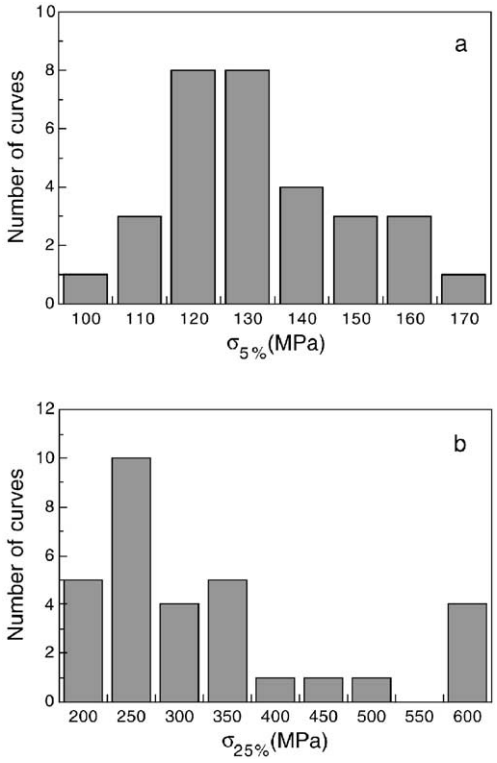

Fig. 3. Statistical distribution of two of the parameters used to describe the stress–strain curves of *A. trifasciata* drag line. (a) $\sigma_{5\%}$ (example of a parameter characterising the initial stages of tensile deformation), and (b) $\sigma_{25\%}$ (example of a parameter characterising the later stages of tensile deformation). The coefficient of variation in (b) is significantly greater than in (a).

use $\sigma_{15\%}$ and $\sigma_{25\%}$ to describe this part of the stress–strain curve. In all cases, $\sigma_{25\%}$ lies below the tensile strength of the sample, which serves as a final and necessary parameter in our attempted fit.

3.4. Statistical distribution of the mechanical parameters

Our next step in this analysis involves determining the statistical distribution of each individual parameter. Examples of the plots used in this procedure are presented in Fig. 3(a) and (b), representing the distribution of the values of $\sigma_{5\%}$ and $\sigma_{25\%}$, respectively. In each case, the range of values taken by the parameter is divided into intervals of equal width (10 MPa for $\sigma_{5\%}$ and 50 MPa for $\sigma_{25\%}$), and the number of tensile tests in which the value of that parameter lay within a given interval is determined. The mean value, standard deviation, and Pearson's coefficient of variation [23] are calculated for each distribution and are presented in Table 2.

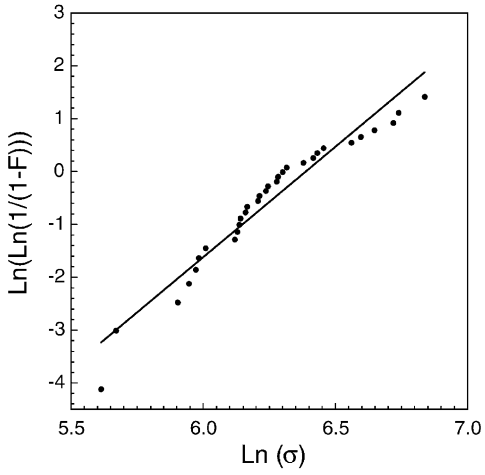

Fig. 4. Weibull plot constructed from tensile strength measurements performed on 31 samples of *A. trifasciata* drag line.

The coefficients of variation show that the properties characterised in the later stages of tensile deformation ($\sigma_{15\%}$, $\sigma_{25\%}$, σ_u) are markedly more variable than those pertaining to the initial stages (E, σ_y, $\sigma_{5\%}$). This distinction is also qualitatively evident in Fig. 1. We can conclude that there is greater scope for tailoring the viscoplastic response and tensile strength of drag line and its analogues, compared to the elastic modulus and the yield strength. Which of these can be tailored *independently* will be explored in Section 3.5.

The tensile strength variability has also been quantified via a conventional Weibull analysis to allow direct comparison with the results of previous studies on silks [7,18,24]. The Weibull plot [25] is presented in Fig. 4, where the data are fitted by a straight line that has a slope of 4.0 ± 0.1 (the Weibull modulus m) and an extrapolated y-axis intercept of 574 ± 1 MPa (a measure of the average tensile strength of the material). Low values of m are synonymous with a highly variable tensile strength; for example, $5 \leq m \leq 25$ for earthenware and other common ceramics, but $200 \leq m \leq 300$ for typical ductile metals. Previous studies

Table 2
Statistical data for individual mechanical parameters

Parameter	Mean value	Standard deviation	Coefficient of variation[a] (%)
E (GPa)	7	1	14
σ_y (MPa)	126	22	17
$\sigma_{5\%}$ (MPa)	132	17	13
$\sigma_{15\%}$ (MPa)	194	71	37
$\sigma_{25\%}$ (MPa)	334	154	46
σ_u (MPa)	540	159	29

[a] Standard deviation divided by mean value and expressed as a percentage [23].

Table 3
Analysis for statistical independence of the mechanical parameters. The number in roman font gives the value of X^2; the number in italic font gives the value of the $\chi^2_{0.95}$ function

	σ_y	$\sigma_{5\%}$	$\sigma_{15\%}$	$\sigma_{25\%}$	σ_u
E	36.1 < *46.2*; independent	32.2 < *41.3*; independent	45.8 < *50.9*; independent	35.5 < *46.2*; independent	34.9 < *36.4*; independent
σ_y		64.0 < *74.5*; independent	90.4 < *92.8*; independent	75.1 < *85.7*; independent	42.8 < *65.2*; independent
$\sigma_{5\%}$			52.2 < *90.5*; independent	43.1 < *74.5*; independent	40.6 < *58.1*; independent
$\sigma_{15\%}$				146.2 > *92.8*; dependent	64.5 < *72.2*; independent
$\sigma_{25\%}$					64.8 < *65.2*; independent

of silkworm cocoon fibre [18,24] and spider drag line [7] have consistently yielded values of m in the range 3–6, suggesting that these silks would not function as reliable engineering materials.

3.5. Statistical correlation of the mechanical parameters

We now explore whether there is any correlation between the different parameters, and whether any functional dependence can be established between them. This problem is equivalent to determining the minimum set of parameters required for a full description of the stress–strain curve.

The range of values taken by each parameter is divided into intervals of equal width, and histograms are constructed, as described in Section 3.4. The test of independence [26] requires the following function to be computed for each pair of parameters

$$X^2 = \sum_{i=1}^{k}\sum_{j=1}^{l}\frac{(n_{ij} - np_iq_j)^2}{np_iq_j} \quad (1)$$

where n is the total number of tensile tests; $k(l)$, the number of intervals into which the range of values of the first (second) parameter is divided; n_{ij}, the number of tensile tests for which the first parameter lies in the interval i and the second parameter lies in the interval j,

$$p_i = \frac{1}{n}\sum_{j=1}^{l} n_{ij} \qquad q_j = \frac{1}{n}\sum_{i=1}^{k} n_{ij}$$

The value of X^2 is compared with the tabulated value of the $\chi^2_{1-\alpha}$ function. The appropriate number of degrees of freedom for $\chi^2_{1-\alpha}$ is given by the product $(k-1)(l-1)$, and the level of significance α is assigned a value of 5% in keeping with common practice [26]. If $X^2 > \chi^2_{0.95}$, the independence hypotheses has to be rejected. Results are presented in Table 3, from which it is apparent that the only pair of parameters with a statistically significant correlation is $\sigma_{15\%}/\sigma_{25\%}$.

One of our stated aims in this work is to determine the *minimum* number of parameters that will adequately describe the stress–strain curves of drag line. It therefore is necessary to check whether the statistical correlation between $\sigma_{15\%}$ and $\sigma_{25\%}$ can be expressed as a clear functional dependence. Fig. 5(a) displays the ($\sigma_{15\%}$, $\sigma_{25\%}$) pairs gleaned from all 31 tensile tests. A strongly linear relationship is evident, with the correlation coefficient R equal to 0.97. Similarly and generally, values of σ associated with *any* particular fixed value of strain in the hardening region can be shown to have a strong linear correlation to the corresponding values of $\sigma_{15\%}$. In contrast, Fig. 5(b) shows the relationship between σ_y and σ_u, which according to the test in Table 3 are statistically independent, and for which an attempted linear fit yields $R = 0.05$.

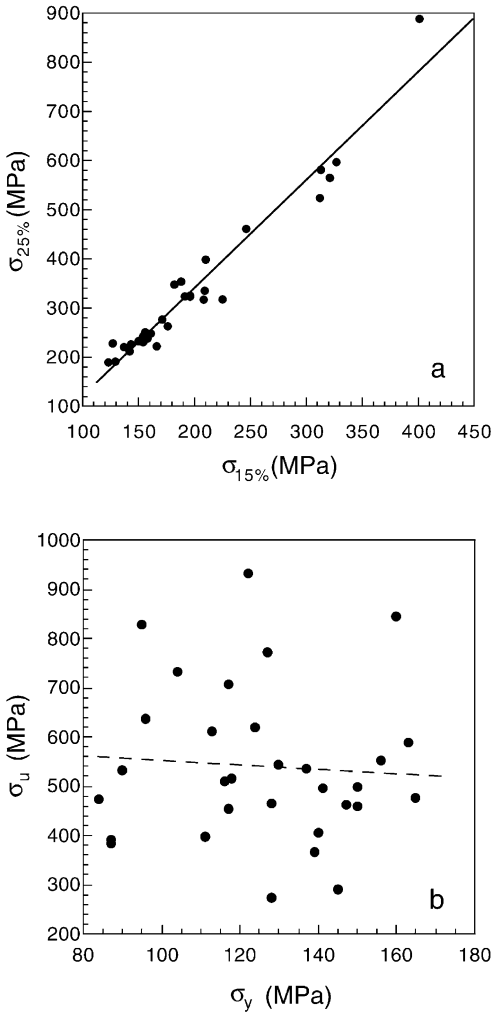

Fig. 5. (a) Scatter diagram showing ($\sigma_{15\%}$, $\sigma_{25\%}$) pairs collected from tensile tests performed on 31 samples of *A. trifasciata* drag line. (b) Scatter diagram showing (σ_y, σ_u) pairs collected from tensile tests performed on 31 samples of *A. trifasciata* drag line. In each case, the straight line shows the result of a linear regression analysis.

3.6. Reconstruction of the stress–strain curves

The preceding discussion leaves us with five independent parameters: E, σ_y, $\sigma_{5\%}$, $\sigma_{15\%}$ and σ_u. We now consider how successful these are at representing (reconstructing) entire stress–strain curves.

It is convenient to divide each stress–strain plot into four segments for this purpose. The segments map simply onto the linear elastic, yield, and hardening regions (defined in Fig. 2 and its accompanying text):

(A) The first segment fits the linear elastic region.
(B) The second and third segments are also approximated by straight lines; together they describe the yield region. They respectively accommodate the new slope of the stress–strain plot beyond σ_y, and any subsequent regime of near-constant stress.
(C) The fourth segment corresponds to the hardening region, where stress increases non-linearly with strain. We can fit this region with a polynomial:

$$\sigma = a_n\varepsilon^n + a_{n-1}\varepsilon^{n-1} + a_{n-2}\varepsilon^{n-2} + \cdots + a_0 \quad (2)$$

We find that a good approximation to the experimental curve is provided by the simplest case, where the polynomial is a quadratic function:

$$\sigma = a\varepsilon^2 + b\varepsilon + c \quad (3)$$

In Section 3.5, we have noted that the hardening region can be described in terms of a single parameter (stress at a fixed strain, e.g. $\sigma_{15\%}$): all the other stresses are related to it through the type of simple correlation illustrated in Fig. 5(a). The coefficients a, b and c in Eq. (3) can therefore be calculated from $\sigma_{15\%}$.

Full details of the procedure for reconstructing stress–strain curves from the independent parameters E, σ_y, $\sigma_{5\%}$, $\sigma_{15\%}$ and σ_u are given in Appendix A.

Fig. 6(a) and (b) compares experimental curves and curves reconstructed following the methodology described earlier. The inserts in both figures show the relative error as defined by the ratio:

$$\frac{\text{(experimental stress)} - \text{(reconstructed stress)}}{\text{experimental stress}}$$

The worst fit occurs in the yield region, where we have approximated the stress–strain characteristics by two straight lines, and at high strains, where the quadratic fit to the hardening region becomes less accurate. The latter error can be reduced to any desired level by using a higher-order polynomial as described in Appendix A. Overall, the mean relative error is less than 5%.

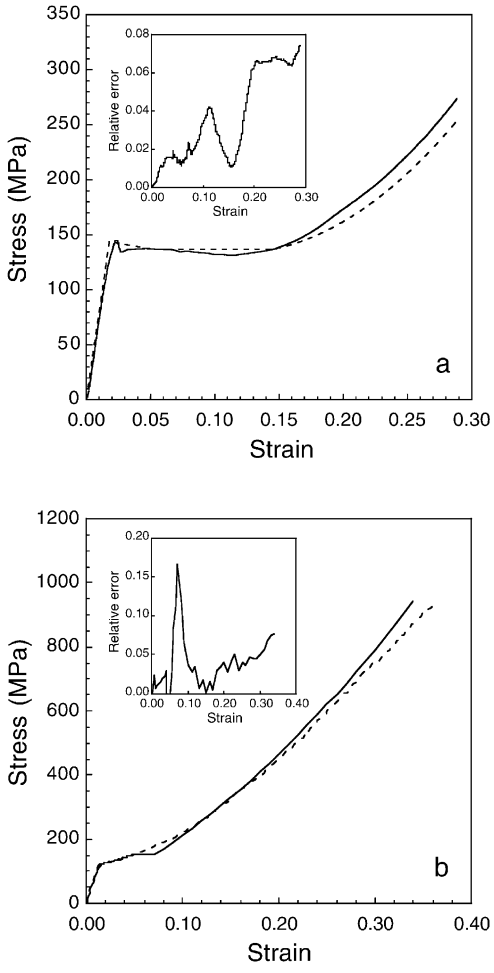

Fig. 6. Comparison of the experimental stress–strain curve (solid line) and reconstructed stress–strain curve (broken line), for two different samples of *A. trifasciata* drag line. Relative error is defined in the text. The samples are representative of behaviour at the (a) low and (b) high ends of the range of tensile strengths exhibited by this type of silk.

4. Conclusions

1. The variability of tensile properties exhibited by naturally spun spider (*A. trifasciata*) drag line under different circumstances can be accounted for at the intraindividual level.
2. The later stages of tensile tests performed on natural drag line (the hardening region) are significantly more variable than the early stages of deformation (the elastic and yield regions). If this behaviour extends to fibres spun artificially from silk-like materials, there is greater scope for tailoring the viscoplastic hardening aspects of their behaviour, in comparison to the initial elastic response.
3. The initial linear elastic response of natural drag line is not significantly correlated to the yield behaviour, and neither of these are significantly correlated to the subsequent viscoplastic hardening. A biomimetic silk spinning process should therefore be able to deliver some degree of independent control of elastic modulus, yield strength, and viscoplastic hardening, within their respective ranges of variability.

4. The experimental stress–strain curves can be represented effectively by just five independent parameters: E, σ_y, $\sigma_{5\%}$, $\sigma_{15\%}$ (or any other value of stress that lies in the hardening region) and σ_u.

Acknowledgements

A. trifasciata specimens were kindly provided by Jesús Miñano (Universidad de Murcia). We thank Oscar Campos and Pablo García (Naturaleza Misteriosa, Parque Zoológico de Madrid) for rearing the spiders, and José Miguel Martínez for help with testing samples and drawing figures. This work was funded by Ministerio de Ciencia y Tecnología (Spain) through project MAT 2000-1334. Additional support was received from the Ministerio de Educación y Cultura (Spain) and the British Council through an Acción Integrada.

Appendix A. Calculation details for reconstructing stress–strain curves

The reconstruction procedure considers the stress–strain curve in four segments. These correspond to the regions A, B and C identified in Fig. 2, with two of the segments accommodated in region B.

(A) Initial linear elastic region ($\sigma = 0 \rightarrow \sigma = \sigma_y$). The stress–strain curve is represented by a straight line of slope E.

(B1) Yield region 1 ($\sigma_y \rightarrow \sigma_{5\%}$). The yield region is approximated by two straight line segments. The first of these embraces the change in slope which occurs in the stress–strain plot beyond σ_y; it extends from the defined point of yield (ε_y, σ_y) to the point (0.05, $\sigma_{5\%}$). Its equation is:

$$\frac{\sigma - \sigma_y}{\varepsilon - \varepsilon_y} = \frac{\sigma_{5\%} - \sigma_y}{\varepsilon_{5\%} - \varepsilon_y} = \frac{\sigma_{5\%} - \sigma_y}{0.05 - \varepsilon_y} \tag{A1}$$

The value of ε_y is provided by Hooke's law:

$$\varepsilon_y = \frac{\sigma_y(\text{MPa})}{E(\text{GPa}) \times 1000}$$

(B2) Yield region 2 (stress remains constant at $\sigma_{5\%}$, while strain increases). The second straight line segment in the yield region takes into account the approximately flat section exhibited by many of the stress–strain curves, and leads into the hardening region at a strain ε_i. The method used to identify the value of ε_i is explained later.

(C) Hardening region ($\sigma_i \equiv \sigma_{5\%} \rightarrow \sigma_u$). As noted in Section 3.6, this region is approximated well by a quadratic function:

$$\sigma = a\varepsilon^2 + b\varepsilon + c \tag{A2}$$

Therefore

$$\begin{aligned}
\sigma_{15\%} &= a\varepsilon_{15\%}^2 + b\varepsilon_{15\%} + c = 0.0225a + 0.15b + c \\
\sigma_{20\%} &= a\varepsilon_{20\%}^2 + b\varepsilon_{20\%} + c = 0.04a + 0.2b + c \\
\sigma_{25\%} &= a\varepsilon_{25\%}^2 + b\varepsilon_{25\%} + c = 0.0625a + 0.25b + c
\end{aligned} \tag{A3}$$

Solution of the simultaneous linear Eq. (A3) leads to:

$$\begin{aligned}
a &= 200\sigma_{15\%} - 400\sigma_{20\%} + 200\sigma_{25\%} \\
b &= -90\sigma_{15\%} + 160\sigma_{20\%} - 70\sigma_{25\%} \\
c &= 10\sigma_{15\%} - 15\sigma_{20\%} + 6\sigma_{25\%}
\end{aligned} \tag{A4}$$

But in Section 3.5 and Fig. 5(a), it was shown that there is a close-to-linear dependence between $\sigma_{15\%}$ and $\sigma_{25\%}$. The equation of the best fit is:

$$\sigma_{25\%} = -92.36 + 2.16\sigma_{15\%} \qquad (R = 0.97) \tag{A5}$$

Near-linear relationships are also found experimentally between $\sigma_{15\%}$ and other values of stress that lie within the hardening region. For example, in the case of the correlation between $\sigma_{15\%}$ and $\sigma_{20\%}$, the equation of the best fit is:

$$\sigma_{20\%} = -55.3 + 1.58\sigma_{15\%} \qquad (R = 0.99) \tag{A6}$$

Substitution of Eqs. (A5) and (A6) into Eq. (A4) provides the coefficients a, b and c in terms of just one independent parameter, $\sigma_{15\%}$:

$$\begin{aligned}
a &= 3648 \qquad b = 11.6\sigma_{15\%} - 2383 \\
c &= -0.74\sigma_{15\%} + 275.3
\end{aligned} \tag{A7}$$

Finally, the strain ε_i, which fixes the lower limit of the hardening region, can be obtained from Eq. (A2)

$$\sigma_i = \sigma_{5\%} = a\varepsilon_i^2 + b\varepsilon_i + c$$

with a, b and c again given by Eq. (A7).

If the hardening region were not adequately represented by a quadratic function, i.e. by Eq. (A2), we could of course use a higher-order polynomial in ε. This would necessitate the calculation of more coefficients, but the approach used earlier could be expanded accordingly by quantifying more linear correlations of the type

$$\sigma_{z\%} = C_z + M_z\sigma_{15\%} \qquad (\sigma_i < \sigma_{z\%} < \sigma_u)$$

It is important to be clear about the difference between the measured coefficients C_z, M_z and the independent measured parameters E, σ_y, $\sigma_{5\%}$, $\sigma_{15\%}$, σ_u. The former are determined on a once-off basis from a representative selection of naturally spun drag line samples. They can then be used together with the independent measured parameters for *any* sample of this material to reconstruct the entire stress–strain curve for that sample to an acceptable level of accuracy.

References

[1] Kaplan DL, Adams WW, Farmer BL, Viney C, editors. Silk polymers: materials science and biotechnology, Washington, DC: American Chemical Society, 1994.

[2] Int J Biol Macromolecules 1999; 24 (parts 2–3; special issue: Silk Symposium).

[3] O'Brien JP, Fahnestock SR, Termonia Y, Gardner KH. Adv Mater 1998;10:1185–95.

[4] Viney C. Silk fibres: origins, nature and consequences of structure. In: Elices M, editor. Structural biological materials, New York/Oxford: Pergamon/Elsevier, 2000. p. 293–333.

[5] Work RW. Text Res J 1976;46:485–92.

[6] Dunaway DL, Thiel BL, Viney C. J Appl Polym Sci 1995;58:675–83.

[7] Pérez-Rigueiro J, Elices M, Llorca J, Viney C. J Appl Polym Sci 2001;82:2245–51.

[8] Madsen B, Shao ZZ, Vollrath F. Int J Biol Macromolecules 1999;24:301–6.

[9] Craig CL, Hsu M, Kaplan D, Pierce NE. Int J Biol Macromol 1999;24:109–18.

[10] Kaplan DL, Lombardi SJ, Muller WS, Fossey SA. Silks: chemistry, properties and genetics. In: Byrom D, editor. Biomaterials: novel materials from biological sources, New York: Stockton Press, 1991. p. 1–53.

[11] Zemlin JC. A study of the mechanical behavior of spider silks. Report number 69-29-CM (AD 684333). Natick, MA: US Army Natick Laboratories, 1968.

[12] Craig CL, Riekel C, Herberstein ME, Weber RS, Kaplan D, Pierce NE. Mol Biol Evol 2000;17:1904–13.

[13] Guess KB, Viney C. Thermochim Acta 1998;315:61–66.

[14] Vollrath F, Madsen B, Shao ZZ. Proc R Soc Lond B 2001;268:2339–46.

[15] Garrido MA, Elices M, Viney C, Pérez-Rigueiro J. Polymer 2002;43:1537–40.

[16] Cohen P. New Scientist 10 October 1998: 11

[17] Scheller J, Gührs K-H, Grosse F, Conrad U. Nature Biotechnol 2001;19:573–7.

[18] Pérez-Rigueiro J, Viney C, Llorca J, Elices M. J Appl Polym Sci 1998;70:2439–47.

[19] Pérez-Rigueiro J, Viney C, Llorca J, Elices M. J Appl Polym Sci 2000;75:1270–7.

[20] Work RW. Text Res J 1977;47:650–62.

[21] Dunaway DL, Thiel BL, Srinivasan SG, Viney C. J Mater Sci 1995;30:4161–70.

[22] Elias H-G. An introduction to polymer science. Weinheim: VCH, 1997.

[23] Moroney MJ. Facts from figures. Harmondsworth, UK: Penguin Books, 1977.

[24] Pérez-Rigueiro J, Elices M, Llorca J, Viney C. J Appl Polym Sci 2001;82:1928–35.

[25] Chou T-W. Microstructural design of fiber composites. Cambridge, UK: Cambridge University Press, 1992.

[26] Brandt S. Statistical and computational methods in data analysis. Amsterdam: North-Holland, 1983.